

**The assessment of growth kinetics in the intermetallic layers of Al-Al<sub>x</sub>Ni<sub>y</sub>-Ni laminate composites**

Azimi, M.; Toroghinejad, M. R.; Shamanian, M.; Kestens, L. A.I.

**DOI**

[10.1088/1742-6596/1270/1/012026](https://doi.org/10.1088/1742-6596/1270/1/012026)

**Publication date**

2019

**Document Version**

Final published version

**Published in**

Journal of Physics: Conference Series

**Citation (APA)**

Azimi, M., Toroghinejad, M. R., Shamanian, M., & Kestens, L. A. I. (2019). The assessment of growth kinetics in the intermetallic layers of Al-Al Ni -Ni laminate composites. *Journal of Physics: Conference Series*, 1270(1), Article 012026. <https://doi.org/10.1088/1742-6596/1270/1/012026>

**Important note**

To cite this publication, please use the final published version (if applicable). Please check the document version above.

**Copyright**

Other than for strictly personal use, it is not permitted to download, forward or distribute the text or part of it, without the consent of the author(s) and/or copyright holder(s), unless the work is under an open content license such as Creative Commons.

**Takedown policy**

Please contact us and provide details if you believe this document breaches copyrights. We will remove access to the work immediately and investigate your claim.

PAPER • OPEN ACCESS

## The assessment of growth kinetics in the intermetallic layers of Al-Al<sub>x</sub>Ni<sub>y</sub>-Ni laminate composites

To cite this article: M Azimi *et al* 2019 *J. Phys.: Conf. Ser.* **1270** 012026

View the [article online](#) for updates and enhancements.



**IOP | ebooks™**

Bringing you innovative digital publishing with leading voices to create your essential collection of books in STEM research.

Start exploring the collection - download the first chapter of every title for free.

# The assessment of growth kinetics in the intermetallic layers of Al-Al<sub>x</sub>Ni<sub>y</sub>-Ni laminate composites

M Azimi.<sup>1,2,3\*</sup>, M R Toroghinejad<sup>1</sup>, M Shamanian<sup>1</sup>, L A I Kestens<sup>2,3</sup>

<sup>1</sup>Dept. of Materials Engineering, Isfahan University of Technology, Isfahan, Iran;

<sup>2</sup>EEMMeCS Dept., Metals Science and Technology Group, Ghent University, Ghent, Belgium;

<sup>3</sup>Dept. of Materials Science Engineering, Delft University of Technology, Delft, The Netherlands

\*Email: [M.Azimi@tudelft.nl](mailto:M.Azimi@tudelft.nl), [M.Azimi@iut.ma.ac.ir](mailto:M.Azimi@iut.ma.ac.ir); [Monireh.Azimi@ugent.be](mailto:Monireh.Azimi@ugent.be)

**Abstract.** Ni aluminides have technologically attracted much attention as oxidation protective layers on Ni-superalloys for high-temperature and harsh environments applications as well as for reinforcements in metal-matrix composites. Among the Ni aluminides, the AlNi compound exhibits the best combination of oxidation-protective characteristics and hardness; thus there is a progressive demand to produce it particularly through convenient in-situ fabrication processes. Therefore, the evaluation of growth kinetics in Al<sub>x</sub>Ni<sub>y</sub> layers is of crucial importance in determining an optimum compound formation process. To this purpose, Al-Ni intermetallic laminate composites were produced through cold roll bonding and subsequent annealing of aluminum and nickel sheets. The microstructure of the intermetallic layers was investigated in order to specify the controlling mechanisms and subsequently the growth model of the different phases. The Al<sub>3</sub>Ni layer was kinetically the first to appear but started to decompose at the expense of the AlNi compound when the direct source of Al disappeared for the reactive diffusion couples. The Al<sub>3</sub>Ni layer growth was initially controlled by bulk diffusion, but then at T ≥ 525°C was modified as a function of competition between formation and consumption, whereas the AlNi growth was governed strongly by the interfacial reaction. The time dependence of the growth rate revealed different behaviors of linear and parabolic kinetics. The overall assessment revealed a bulk diffusion-controlled growth for all of the intermetallic layers. Arrhenius parameters could be derived for the Al<sub>3</sub>Ni layer, while it was impossible for the AlNi phase because the formation of this layer was caused by a mixture of diffusion mechanism.

## 1. Introduction

Between nickel aluminides, the AlNi intermetallic phase exhibits the best combination of oxidation-protective characteristics and hardness, which provokes a great interest in Al-AlNi-Ni composites. Metal-intermetallic laminates (MIL) composites have the potential to combine various functions, which may be of use for high-temperature structural applications such as heat exchangers, which require appropriate thermal management [1,2].

There are some inconsistencies in the data on the growth kinetics of intermetallic phases. For instance, according to Michaelsen and Barmak [3] the growth of Al<sub>3</sub>Ni phase indicates a parabolic dependence on the annealing time, whereas Jung et al [4] have reported that the growth kinetics of Al<sub>3</sub>Ni phase does not obey the parabolic law. Moreover, researchers have reported conflicting results on Al and Ni asymmetric interdiffusion coefficient. Hence, the dominant diffusing element during the



formation of intermetallic phases is still entirely unclear under similar process conditions [2,5–7]. However, Al<sub>3</sub>Ni phase was recognized as the first kinetically favored intermetallic phase, independently of the concentration gradient [5] and imposed strain level [8].

Therefore, a more detailed examination of the formation mechanism of intermetallic phases is of crucial importance to better control the processing of these materials and the aim of this work is to investigate the formation mechanisms and growth kinetics of intermetallic phases in the Al-Ni diffusion couple fabricated by the roll bonding process.

## 2. Experimental procedure

Commercially pure aluminum and nickel were used as initial materials in sheet form. An Al-Ni-Al sandwich was subjected to cold roll bonding (CRB) by 90% reduction in thickness. The details of materials and CRB process were given elsewhere [8]. In order to form Al<sub>x</sub>Ni<sub>y</sub> intermetallic compounds, the cold roll bonded composite with the dimensions of 200 × 60 × 0.5 mm<sup>3</sup> was annealed in the temperature range of 300 to 640 °C for 1 and 4 hours.

In addition to a conventional optical microscopy (OM, Olympus) the microstructural evolution was monitored with a field emission gun scanning electron microscope (FEG-SEM Quanta-450®, FEI) equipped with EBSD facility of type TSL-EDAX® and an energy dispersive spectrometer (EDS).

The microstructure of Al/Ni interface was identified by observing sites of size (100-400 μm) × (30-150 μm). Kikuchi band indexing in EBSD were acquired with OIM™ software and gathered at an accelerating voltage of 20 kV, a working distance of 14 to 16 mm with step sizes in the range of 50 to 80 nm. Samples were tilted 70° for acquiring the maximum yield of backscattered electrons. The thickness of the continuous or segmented layers of the intermetallic phases was determined at several points of the formed layers using image analysis software (ImageJ2)

## 3. Results and discussion

Figure 1 shows BSE images of intermetallic laminate composites obtained through annealing. The intermetallic layer(s) was formed along the Al/Ni original interface, visibly present except for the samples annealed at 300°C. Figure 2a and b shows the dimensions of the intermetallic layers as a function of temperature. The layers are mainly composed of Al<sub>3</sub>Ni and AlNi compounds according to the phase analysis results listed in Table 1. This table also reveals that other compounds possess relatively negligible thickness.

Table 1. Various phase zones which were detected across Al-Ni interface in TD plane of samples using EDS and Kikuchi band indexing in EBSD.

Zone	Average of Spectrums in EDS		Probable phases	Indexed results in EBSD with confidence index (CI)	Confirmed phases	Ave. thickness of reacted zones (μm)
	Al at.%	Ni at.%				
(A)	1.3	98.7	Nickel	well-indexed nickel, CI=0.8	Nickel	Base metal
(B)	17	83	Diffusion zone	well-indexed (Ni), CI= 0.8	Ni-riched solid solution	~0.5
(C)	30.1	69.9	AlNi <sub>3</sub> or (AlNi <sub>3</sub> +Al <sub>3</sub> Ni <sub>5</sub> )	well-indexed AlNi <sub>3</sub> , CI=0.75 not indexed Al <sub>3</sub> Ni <sub>5</sub> , CI=0.03	AlNi <sub>3</sub>	~0.5
(D)	55.3	44.7	(Al <sub>3</sub> Ni <sub>2</sub> +AlNi) or Al <sub>3</sub> Ni <sub>2</sub>	indexed grains as AlNi, CI= 0.3 indexed grains as AlNi <sub>3</sub> , CI= 0.41 not indexed Al <sub>3</sub> Ni <sub>2</sub> , CI=0.01	Mixture of AlNi <sub>3</sub> +AlNi	Various (0-1.6)
(E)	48.3	51.7	AlNi	well-indexed, CI= 0.49	AlNi	Various (0-20)
(F)	76.8	23.2	Al <sub>3</sub> Ni	well-indexed, CI= 0.3	Al <sub>3</sub> Ni	Various (0-9)
(G)	100	0	Al	well-indexed nickel, CI=0.7	Aluminum	Base metal

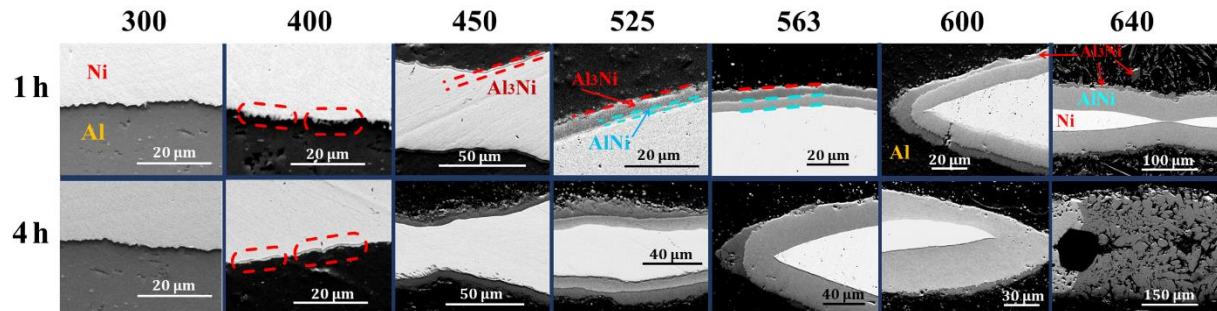


Figure 1. BSE-SEM images of interfaces on TD section of CRB-processed composites after annealing at various times and temperatures.

As shown in Figure 1, the Al phase was melted at 640°C and the interface reactions were no longer solid state. Hence, this temperature data are not given in next results.

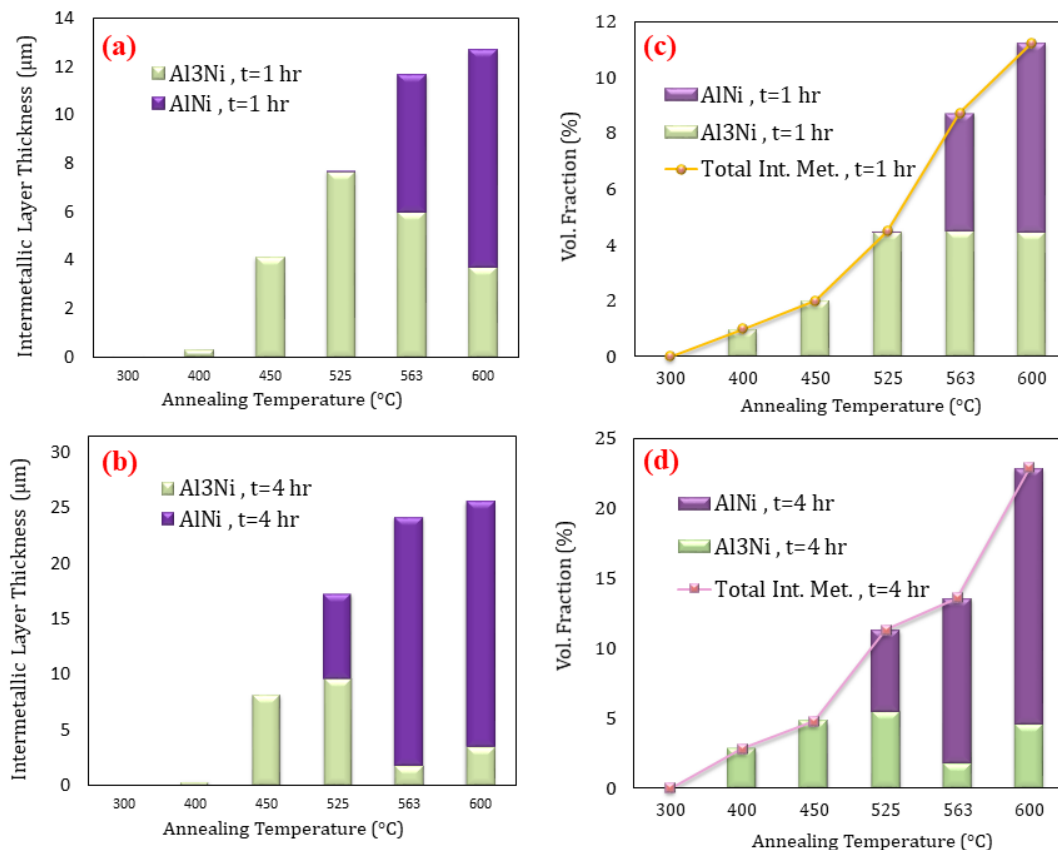


Figure 2. Intermetallic layer thickness/volume fraction vs. temperature during 1 h (a, c) and 4 h (b, d) annealing.

Based on the general empirical equation (1) proposed by Kidson [9], it is possible to model the growth of the thickness of a layer:

$$W_i = kt^n \quad (1)$$

$$\ln(W)_i = n \cdot \ln(t) + \ln(k) \quad (2)$$

whereby  $W_i$  represents the thickness of layer  $i$ ;  $k$ = the growth rate constant;  $t$ = time [min] and  $n$ = kinetics exponent. From a double logarithmic plot,  $n$  and  $k$  values can be derived from a linear fit of the

experimental data (cf. Figure 3). However, the accuracy of the results (cf. Table 2) may be influenced by the only two values of the time.

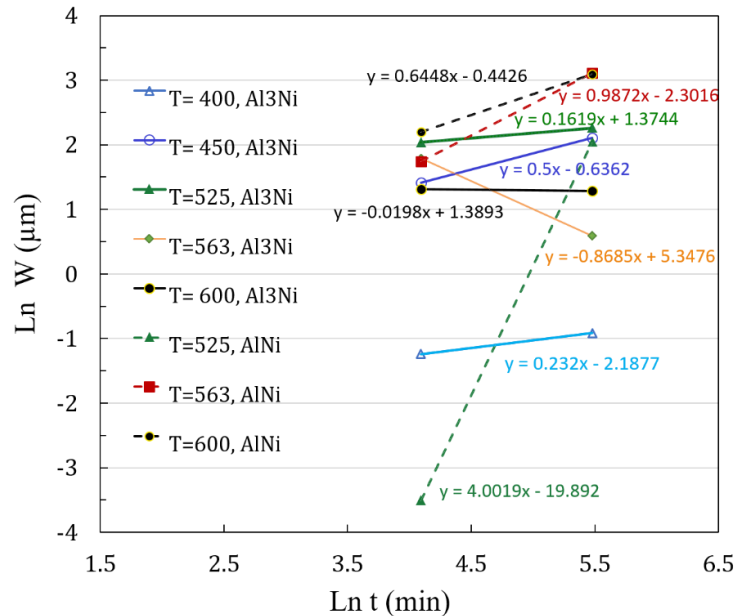


Figure 3.  $\text{Ln}W_i$  versus  $\text{Ln}t$  for  $\text{Al}_3\text{Ni}$  and  $\text{AlNi}$  compounds.

Table 2. Growth kinetics parameters of  $n$  and  $k$  in  $\text{Al}_3\text{Ni}$  and  $\text{AlNi}$  layers.

Kinetics parameters		$T(^{\circ}\text{C})$				
		400	450	525	563	600
$n$	$\text{Al}_3\text{Ni}$	0.38	0.5	0.16	-0.81	-0.02
	$\text{AlNi}$	-	-	4.00	0.99	0.65
$\text{Ln } k$	$\text{Al}_3\text{Ni}$	-2.19	-0.64	1.37	5.35	1.39
	$\text{AlNi}$	-	-	-19.89	-2.30	-0.44
$k$	$\text{Al}_3\text{Ni}$	0.12	0.53	3.95	180.10	4.01
	$\text{AlNi}$	-	-	2.30	1.00	0.64

The factor  $n$  is associated with the controlling mechanism of the intermetallic layer growth process. In terms of quantitative assessment,  $n=1$  demonstrates interfacial reaction controlled growth;  $n=0.5$ : bulk diffusion controlled growth and  $n=0$  corresponds to a balance between the layer formation and decomposition during a secondary reaction.

Intermetallic layers may exhibit different behaviors, i.e. sequential growth, concurrent growth and layer shrinkage through decomposition. The last one was observed from  $563^{\circ}\text{C}$  onward, owing to the fact that  $\text{Al}_3\text{Ni}$  (i.e. the Ni-poorest intermetallic) had already started to be consumed at expense of the  $\text{AlNi}$  compound when the  $\text{Al}$  direct source disappears from the reactive diffusion couples. Up to  $450^{\circ}\text{C}$ , only  $\text{Al}_3\text{Ni}$  layer was formed and afterwards followed the second stage of a two-stage growth process. The parabolic growth kinetics suggests bulk diffusion controlled growth until the growth kinetics is disturbed by the emerging new  $\text{AlNi}$  phase at  $T \geq 525^{\circ}\text{C}$  (the volume fraction of intermetallic layers readily indicates a change in the trend due to this disturbance, cf. Figures 2 c, d). Indeed, a part of the  $\text{Al}_3\text{Ni}$  layer is consumed through the reaction at the  $\text{Al}_3\text{Ni}/\text{Ni}$  interface, cf. Equation 3. Eventually, the growth rate is a function of the competition between  $\text{Al}_3\text{Ni}$  direct formation by diffusion and consumption by the interfacial reaction, while the new phase ( $\text{AlNi}$ ) growth is strongly controlled by the interfacial reaction.



Afterwards, increasing the temperature by only  $\sim 40^\circ$  ( $T=563^\circ\text{C}$ ) results in a further increase of the relative thickness/fraction of the AlNi layer. In this stage, AlNi growth kinetics is linear, still controlled by the reaction (equation 3) at  $Al_3Ni/AlNi$  interface, but not as strong as that of at the lower temperature ( $525^\circ\text{C}$ ). In the meanwhile, the  $Al_3Ni$  decomposition rate prevailed the formation rate at the  $Al/Al_3Ni$  interface. After that, increasing the temperature close to the melting point of Al, the atomic mobility is promoted accelerating bulk diffusion. On the one hand, it results in a balance between  $Al_3Ni$  phase consumption and formation rate, giving rise to constant growth kinetics, while on the other hand, it leads to parabolic growth kinetics of the AlNi layer. This parabolic function implies that the AlNi growth dependency on the reaction has subsided.

The growth rate constant  $k$  is an exponential function of the temperature variable, cf. equation 4. Whereby  $Q$  is the activation energy for diffusion-limited growth and  $k_0$  represents an independent factor of time and temperature and  $R$ = the global gas constant.

$$k = k_0 \exp\left(\frac{-Q}{RT}\right) \quad (4)$$

$$\ln k = \ln(k_0) - \frac{Q}{RT} \quad (5)$$

By combining equations (1) and (4), equation (6) is obtained as follows:

$$W = f(T, t, n) = k_0 t^n \exp\left(\frac{-Q}{RT}\right) \quad (6)$$

Defining the B parameter as equation (7),  $W$  is a function of temperature according to equation (8) (for constant values of  $n$  and  $t$ ).

$$B = f(t, n) = k_0 t^n \quad (7)$$

$$W = f(T) = B \exp\left(\frac{-Q}{RT}\right) \quad (8)$$

Table 3. B function according to n values.

Layer - T(°C)	n	B	$\frac{\partial W}{\partial t}$ , growth rate	Considerable remarks
$Al_3Ni$ - 563	-1	$\frac{k_0}{t}$	<0	Layer consumption
$Al_3Ni$ - 525, 600	0	$k_0$	0	Growth depends on temperature, independent of time
$Al_3Ni$ - 400, 450 $AlNi$ - 600	0.5	$k_0 t^{0.5}$	>0	Parabolic kinetics
$AlNi$ - 563	1	$k_0 t$	>0	Linear kinetics
$AlNi$ - 525	4	$k_0 t^4$	>0	Growth depends on interface reaction strongly

Based on the present values for the  $n$  variable, the B function appears in five forms which are listed in Table 3. In both layers, the dependency of B on the time is decreasing with temperature increase, independent of the function form and except at  $600^\circ\text{C}$  for  $B_{Al_3Ni}$ . At  $600^\circ\text{C}$ , this dependency is higher owing to the presence of the thick and compact layer of AlNi, which gives rise to a deceleration of the supply of Ni atoms by the diffusion process in order to form the  $Al_3Ni$  phase.

The  $Q$  value is calculated, cf. Figure 4, under the condition that growth is controlled by diffusion ( $n=0.5$ ). Hence, this calculation is possible for the  $Al_3Ni$  layer in the  $400-450^\circ\text{C}$  range and estimation for AlNi layer in the  $563-600^\circ\text{C}$  range with the least possible error. The estimation here obtained is far from the finding by Urrutia et al [10] because of the mixture of bulk and grain boundary (GB) diffusion for AlNi formation in the present work. This can be explained by the wave-like morphology of the  $Al_3Ni/AlNi$  interface as one might expect from GB diffusion, cf. Figure 5.

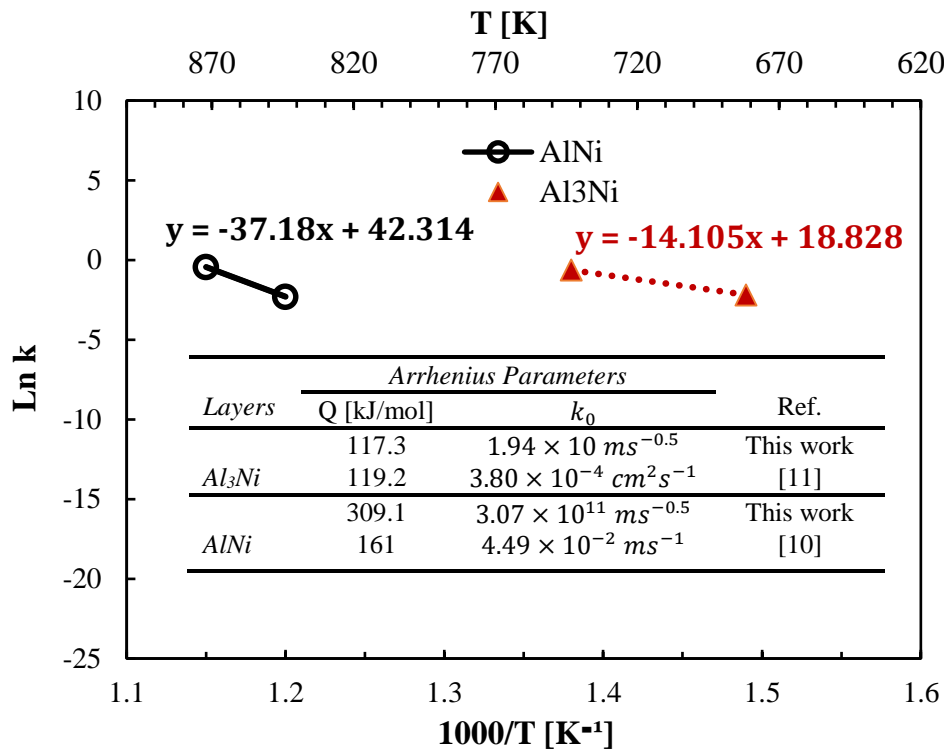


Figure 4.  $\ln k$  versus  $1/T$  plot and the corresponding Arrhenius parameters.

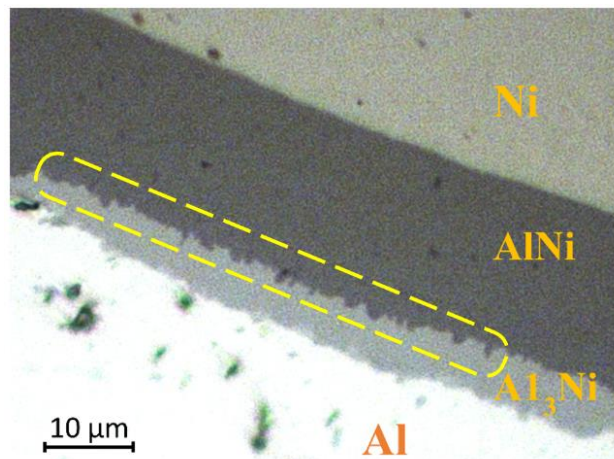


Figure 5. A typical wave-like interface of the  $Al_3Ni/AlNi$  in TD section (the sample was annealed at 600 for 4 h).

The overall growth assessment of intermetallic layers reveals an exponential trend as a function of temperatures, cf. Figure 6, indicating bulk diffusion-controlled growth of layers according to the Arrhenius model. Further, diffusion acceleration via base metals grain boundaries does not play a significant role during layers growth because the cold rolled grains of the base metals have already recrystallized and grown in the first stages of the annealing. After the annealing, Al and Ni grains exhibited the equivalent diameter of 60 and 102  $\mu\text{m}$  from 2.3 and 50  $\mu\text{m}$  in the cold roll-bonded stage, respectively.

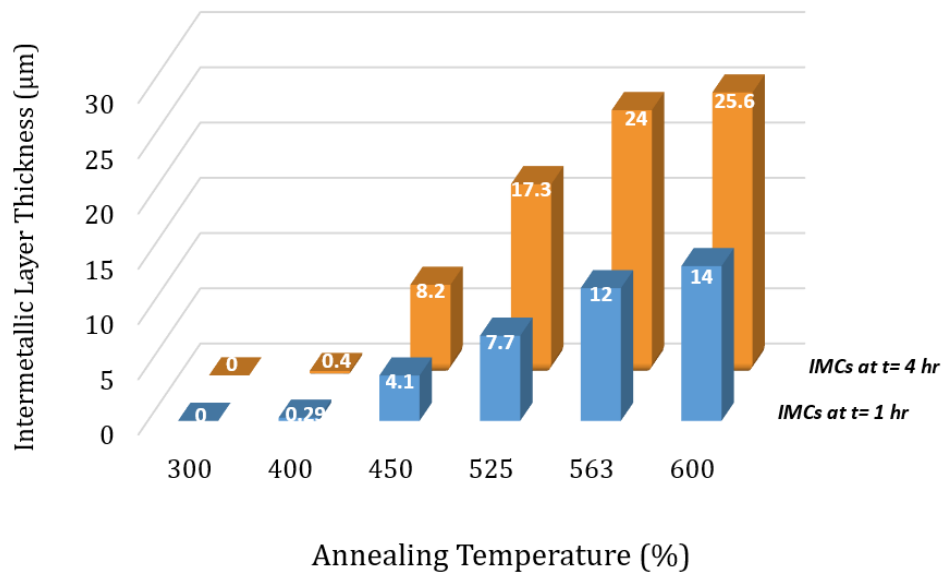


Figure 6. The overall Int. Met. layers thickness vs. annealing temperature during 1 and 4 hours.

#### 4. Conclusion

An Al-AlNi-Ni laminate composite is relatively obtainable by annealing above 560°C longer than 4 h. In the term of growth kinetics and based on the overall assessment, intermetallic layers growth obeys Arrhenius model which indicates bulk diffusion controlled growth. However, internal layers exhibit different behaviors of sequential growth, concurrent growth and layer decreasing through decomposition. Up to 450°C, only Al<sub>3</sub>Ni layer was formed and followed the second stage of a two-stage growth process. By emerging AlNi compound at higher temperatures, Al<sub>3</sub>Ni growth behavior changes to consumption. The AlNi layer formation was controlled by a mixture of bulk and grain boundary diffusion while bulk diffusion was the only mechanism which controls the growth of Al<sub>3</sub>Ni with activation energy similar to the previous studies.

#### References

- [1] Konieczny M 2012 *Mater. Charact.* **70** 117–124
- [2] Srivastava V C, Singh T, Ghosh Chowdhury S and Jindal V 2012 *J. Mater. Eng. Perform.* **21** 1912–1918
- [3] Michaelsen C and K. Barmak K 1997 *J. Alloys Compd.* **257** 211–214
- [4] Jung S, Minamino Y, Yamane T and Saji S 1993 *J. Mater. Sci. Lett.* **12** 1684–1686
- [5] Sauvage X, Dinda G P and Wilde G 2007 *Scr. Mater.* **56**, 181–184
- [6] Vojtěch D, Novák M, Zelinková M, Novák P, Michalcová A and Fabián T 2009 *Appl. Surf. Sci.* **255** 3745–3751
- [7] Liu J C, Mayer J W and Barbour J C 1988 *J. Appl. Phys.* **64** 651–655
- [8] Azimi M, Toroghinejad M R, Shamanian M and Kestens L A I 2017 *Metals* **7** 1–14
- [9] Kidson G 1961 *J. Nucl. Mater.* **3**, 21–29
- [10] Urrutia A, Tumminello S, Aricó S F and Sommadossi S 2014 *CALPHAD Comput. Coupling Phase Diagrams Thermochem.* **44** 108–113
- [11] Ren X, Chen G, Zhou W, Wu C and Zhang J 2009 *J. Wuhan Univ. Technol. Sci. Ed.* **24** 787–790